Elastic Constants in RbI, Determined by Inelastic Neutron Scattering*

A. Loidl[1], J. Daubert[2], and M. Müllner[3]

[1] Institut für Physik, Johannes-Gutenberg-Universität, Mainz
[2] Fachbereich Physik, Technische Universität, München
[3] Institut für Kernphysik, Johann-Wolfgang von Goethe-Universität, Frankfurt

Long-wavelength acoustic phonons have been studied in the whole (100)-plane of RbI at 295 K by means of inelastic neutron scattering. The raw data have been corrected for resolution effects taking into account the curvature of the dispersion surface and variations of the mode eigenvectors. The shifts of the neutron groups due to these resolution effects are discussed in detail. The analysis of the experimental results gives for the zero sound elastic constants $c_{11} = 28.15 \pm 0.5$, $c_{12} = 3.7 \pm 0.5$ and $c_{44} = 2.85 \pm 0.1$ 10^{10} dyn/cm^2. A comparison with first sound elastic constants taken from ultrasonic measurements yields significant differences between the high and low frequency elastic constants c_{11} and $c'' = (c_{11} - c_{12})/2$. The differences calculated from recent theories are in agreement with the experimental results for the elastic constants c_{11}, c_{44} and c'', but not for c_{12}. The dispersion surface in the (100)-plane is also shown for some out-of-symmetry data and compared with ultrasonic data as well as with theoretical results.

I. Introduction

It is well established, that the low and the high frequency elastic constants are different in real crystals. The difference arises because of the interaction of the elastic wave with other excitations in the crystal. This interaction depends on the frequency of the elastic wave [1-3]. In ultrasonic experiments the frequency is usually much less than the averaged inverse lifetime of the thermal phonons in the crystal; this yields first sound elastic constants. At the higher frequencies of a neutron experiment the acoustic wave propagates in the zero sound mode.

In Alkali-Halide crystals with fcc structure zero and first sound elastic constants were calculated by Cowley [1] for NaI, KBr and KI and by Loidl et al. [4] for RbI and NaF. These calculations predict differences between zero and first sound elastic constants of up to 15% at room temperature. There is experimental evidence, that the long wavelength acoustic neutron data deviate from adiabatic sound velocities [5-8], although these measurements did not really aim to

investigate the long wavelength low-frequency region of the phonon dispersion. Taking the data available only a rough comparison with theoretical predictions is possible.

The difference in the temperature gradients of zero and first sound was observed by Svenson and Buyers [9] in KBr, who compared ultrasonic and neutron data at 95 K and 463 K. The experimental result was in rough agreement with Cowley's theory [1]. Recently Loidl et al. [10] performed neutron experiments in NaF at elevated temperatures covering the transition region between zero and first sound. The experimental results were in good agreement with the calculations [4].

The purpose of this work was to make precise neutron measurements at room temperature, to determine the zero elastic constants as well as the dispersion of zero sound in off-symmetry directions. RbI was chosen for two reasons:

Firstly, Raunio and Rolandson [8] reported large deviations of the elastic constants measured by inelastic neutron scattering from ultrasonic data, which reached as much as 30% in c_{12} and c_{44} at 80 K. Secondly, the

microscopic Grüneisen parameters, which determine the coupling constants of the long wavelength mass operators, have been investigated theoretically by Kress and Jex [11–13] and experimentally by Blaschko et al. [14]. So the calculations of the zero sound elastic constants could be based on realistic microscopic coupling parameters.

II. Measurements

A. Experimental Details

The measurements were made using the time-of-flight spectrometer IN7 at the high-flux reactor at the ILL, Grenoble. A monochromatic neutron beam selected by a pyrolytic graphite double monochromator and chopped with a pseudostatistical chopper [15] struck the RbI single crystal. The scattered neutrons were counted at well defined angles in 10 ^{3}He detectors. The flight path between sample and detector was 4m. The time-of-flight spectrum of each detector was recorded in an on-line computer. The collimation between monochromator and sample measured 0.5° horizontally and 0.4° vertically. The widest collimation between sample and detector was 0.45° horizontally and 1.3° vertically, which for some runs was restricted to 0.35° horizontally and 0.25° vertically. We used incident energies of 4.13, 5.0, 5.85, 8.04, 9.70, 16.51, 20.0 and 23.39 meV. Some preliminary measurements were made at the 2m time-of-flight spectrometer at the research reactor FR2 of the Kernforschungszentrum Karlsruhe, also using a pseudostatistical chopper. There the incident energy of 17.68 meV was produced by means of a (0002) reflection from a Be-monochromator and collimations between monochromator and sample were 0.5° horizontally and 0.65° vertically, while the collimations between sample and detector were 0.7° horizontally and 1.7° vertically. The same single crystal of RbI was used throughout this work. It was cylindrical and had the (001) axis within 3° of its geometrical axis. Its diameter and height were 40 mm and 30 mm respectively. The mosaic spread was about 20′.

B. The Determination of Experimental and Intrinsic Peak Positions

The peak position of a neutron group is determined in a straightforward manner using the centre of the full width at half maximum (FWHM) above the background level. For most neutron groups one tenth of this linewidth is a conservative estimate of the uncertainty of the experimental peak position.
The observed lineshape is a convolution of the intrinsic

lineshape and the instrumental resolution. Especially for long-wavelength low-energy modes, two effects require careful corrections

(i) the spectrometer resolution function embraces a whole region in wave-vector space, over which the dispersion relation varies in an anisotropic non-linear manner. This introduces an asymmetry and shifts the centre of the observed neutron groups.

(ii) the variation of the one phonon neutron-scattering cross section across the energy spread of the observed neutron groups shifts the peak-positions towards lower energies.
These effects can be calculated by convoluting the spectrometer resolution function with the dispersion of the frequencies in the region appropriate to the measurements. A meaningful method to do so is one where the actual dispersion surface is numerically integrated over the resolution function of the spectrometer for each time channel. The scattered intensities from the phonons found for a certain spectrometer setting are weighted with the neutron scattering cross section. As our measurements were restricted to the long-wavelength acoustic branches, we calculated the phonon frequencies and eigenvectors with a model of the lattice dynamics in a long-wavelength approximation, which is only determined by the elastic constants.
To compare the results of this computer simulation of scattered intensities with experimental data, we have to convolute the evaluated intensity distribution with the time-of-flight spread, which is determined by the chopper window and the time-of-flight spreads in the sample and in the detector. These contributions were calculated following Furrer [16].
Finally, the results are transformed from an energy to a time-scale.
To show the quality of this simulation we compare in Figure 1 experimental neutron groups with calculated intensities. We used as input parameters both, first sound elastic constants and theoretical zero sound elastic constants [4]. Only the simulation using zero sound elastic constants gave a good agreement, whereas first sound input data yield the centre of the neutron group 0.1 rad THz to low in the LA branch, while the difference in the TA branch is not detectable. In the TA branch also the lineshape is well described.
A further test for the quality of this analysis was to compare the experimental and the calculated shifts of the centre of peak which occurred for different collimations. We measured neutron groups at the IN7 with an incident energy of 5.00 meV and a spectrometer setting to (2.02, 0, 0) with three different sets of collimations between sample and detector:

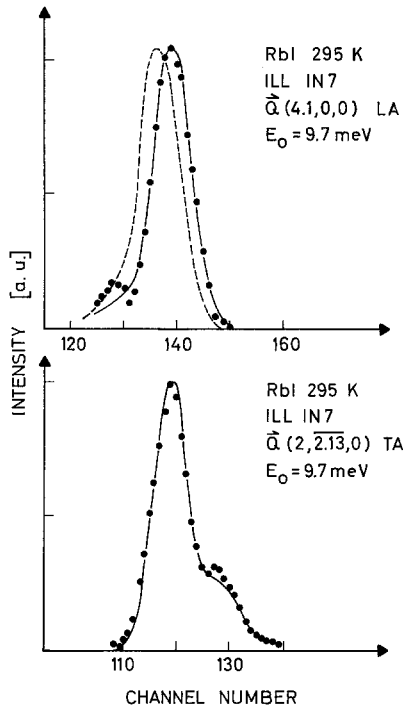a) $\alpha_{hor} = 0.45°$ $\alpha_{ver} = 1.3°$

Fig. 1. Measured and calculated neutron intensities. Neutron data (●) are compared with calculated intensities with elastic constants in the zero sound (———) and in the first sound region (------). In the neutron group with a spectrometer setting to determine a $|\xi 00|$ TA phonon the calculated intensities in the zero and first sound region are nearly identical

b) $\alpha_{hor} = 0.45°$ $\alpha_{ver} = 0.35°$

c) $\alpha_{hor} = 0.35°$ $\alpha_{ver} = 0.25°$.

With the same data we calculated the peak shifts. Table 1 shows the experimental and the calculated shifts of the centre of peaks. The agreement is very satisfactory.

To correct all the experimental data, we did not evaluate for each scattered neutron group the appropriate elastic constants, but we calculated the difference between the peak-positions at finite and at ideal resolutions. For some branches and different experimental settings these corrections are shown in Figure 2. We see that in the $|\xi 00|$ LA branch the corrections are positive (the measured frequencies are too low), but they are very large and negative in the $|\xi 00|$ TA branch. For the time-of-flight spectrometer with two meter flight path, these corrections reach up to 50% of the phonon energy at wave vectors $q/q_{max} = 0.1$ and are still in the order of 15% at $q/q_{max} = 0.3$.

There is still one correction to deal with. In a time-of-flight experiment one measures a distribution of scattered neutron intensities linear over a time scale. We are interested in the phonon-disperion $\omega(q)$, therefore we want to get the experimental data in a linear energy

Table 1. Experimental and calculated peak shifts of measured neutron groups, with three different sets of collimations between sample and detector

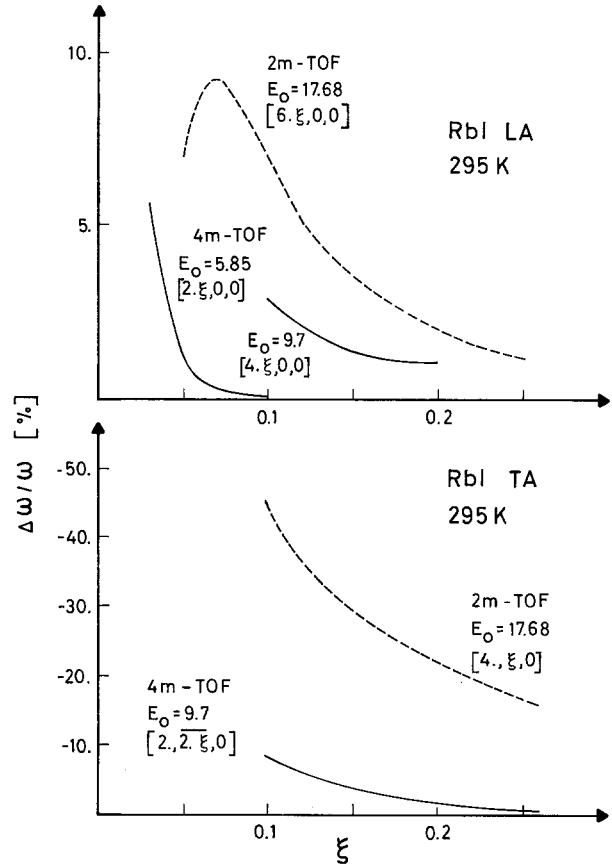|	Δ(a–b)	Δ(a–c)	Δ(b–c)
Exp.	0.5 ± 0.3	-0.6 ± 0.4	-1.1 ± 0.4
Calc.	0.6	-0.4	-1.0

Fig. 2. Resolution correction terms for some branches and different experimental settings in RbI at 295 K

scale. An energy-interval ΔE is proportional to $\Delta t/t^3$. Under the assumption of Gaussian-distributions $Z(t)$, we define the centre of the peak in a linear time scale

$$\bar{t} = \frac{\int_{-\infty}^{+\infty} Z(t) \cdot t \, dt}{\int_{-\infty}^{+\infty} Z(t) \, dt} \tag{1}$$

with

$$Z(t) = \frac{1}{\sqrt{2\pi}\,\sigma} \exp \frac{(t-\bar{t})^2}{2\sigma^2}, \tag{2}$$

where σ is the variance of the distribution.

In a scale weighted with t^3 the centre of the peak is defined

$$\bar{t}' = \frac{\int\limits_{-\infty}^{+\infty} t^3 Z(t)\, t\, dt}{\int\limits_{-\infty}^{+\infty} t^3 Z(t)\, dt}. \tag{3}$$

After a lengthy calculation we get

$$\Delta t = \bar{t}' - \bar{t} = \frac{3\sigma^2(\sigma^2 + \bar{t}^2)}{\bar{t}(3\sigma^2 + \bar{t}^2)} \tag{4}$$

neglecting higher order terms. It should be mentioned, that the elastic peak is shifted, too (Δt_{el}), and the correction is only $\Delta t - \Delta t_{el}$. For small incident energies and especially for measurements with a small neutron energy loss this correction turns out to be quite small.

C. Experimental Results

With the time-of-flight method we measured altogether about 300 neutrons groups in the (100)-plane, most of them in off-symmetry directions. For the analysis we took only data for which corrections were less than 5%.
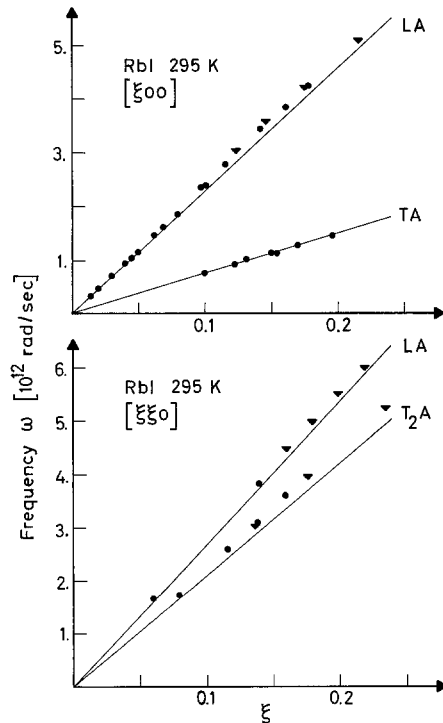

Fig. 3. Long wavelength acoustic phonon frequencies in the $|\xi 00|$ and $|\xi\xi 0|$ main symmetry directions. The measured neutron data of this work (● 4 m flight path, ▼ 2 m flight path) are compared with the extrapolated mean values of the six ultrasonic data (Ref. 17–21)

To get the phonon dispersion in the main symmetry directions we used an interpolation method described by Buyers [5]. In Fig. 3 we present the results in the main symmetry directions and compare our neutron scattering data with a mean value of six ultrasonic measurements [17–22]. The estimated errors are smaller than the symbols used in the figure. The errors in the phonon frequencies were assigned with due regard to the counting statistics and the width and the shape of the neutron groups. For well defined groups the errors were about 5% of the full width at half maximum. Errors in phonon frequency due to errors in the crystal setting have also been calculated and are included in the total error.

In the $|\xi 00|$ LA branch as well as in the $|\xi\xi 0|$ LA and $T_2 A$ branches all measured phonon energies with wave vectors $q/q_{max} > 0.1$ are higher than the extrapolated values determined by ultrasonic techniques, with the most pronounced effect in the $T_2 A$ branch with a sound velocity proportional to $(c_{11} - c_{12})^{1/2}$. In the $|\xi 00|$ TA branch ultrasonic and neutron scattering data agree within the error bars. In the wave vector region $q/q_{max} < 0.1$ the experimental uncertainties are too large to decide whether the phonon frequencies belong to the zero or to the first sound region. With this experiment it was not possible to determine the transition region between zero and first sound, as it has been done in recent experiments in NaF by Loidl et al. [10].

III. Analysis of the Measurements

In this section we describe the analysis of our experimental data. We also compare our results with elastic constants measured by ultrasonic techniques and with the recent theoretical calculations by Loidl et al. [4]. The problem in determining zero sound elastic constants from inelastic neutron data is that one must be sure that the measured frequencies fulfill the condition $\Omega \gg \Gamma$, where Γ is an averaged inverse lifetime of the thermal phonons, and that the influence of the normal negative dispersion of transverse acoustic modes is small. An averaged Γ was deduced from thermal conductivity data to $\Gamma = 0.11$ rad THz [4]. The lowest frequencies we used for the evaluation of zero sound elastic constants were about 1. rad THz. We corrected the influence of the negative dispersion by comparing the long-wavelength data of a Breathing-Shell-Model to the frequencies calculated in a long-wavelength approximation without dispersion using the same elastic constants. These corrections were always less than 2%.

We performed measurements in the whole (100) plane including the (100) and (110) main symmetry directions. From these data it is unambiguously possible to

Table 2. Elastic constants in the first and zero sound regime in RbI at 295 K. The units are 10^{10} dyn/cm^2

Sound regime	c_{11}	c_{44}	$(c_{11}-c_{12})/2$	c_{12}	Ref.
1.	25.83 ± 0.05	$2.78\ \pm0.005$	11.06 ± 0.1	3.7 ± 0.07	[17]
1.	25.60	2.87	11.25	3.1	[18]
1.	25.40 ± 0.05	$2.76\ \pm0.003$	10.67 ± 0.05	4.07 ± 0.02	[19]
1.	25.63 ± 0.13	2.776 ± 0.01	11.27 ± 0.1	$3.4\ \pm0.1$	[20]
1.	25.68 ± 0.05	$2.78\ \pm0.01$	10.94 ± 0.05	$3.8\ \pm0.02$	[22]
1.	25.66 ± 0.03	2.792 ± 0.003	11.02 ± 0.01	3.77 ± 0.006	[21]
1.	25.66 ± 0.1	2.793 ± 0.03	11.01 ± 0.1	3.64 ± 0.15	meanvalue
					This work
0.	$28.0\ \pm0.4$	$2.85\ \pm0.1$	$12.3\ \pm0.3$	$3.3\ \pm0.4$	4m TOF
0.	$28.3\ \pm0.6$		$12.1\ \pm0.5$	$4.1\ \pm0.6$	2m TOF
0.	28.15 ± 0.5	$2.85\ \pm0.1$	$12.2\ \pm0.4$	$3.7\ \pm0.5$	meanvalue

determine the three independent elastic constants c_{11}, c_{12} and c_{44}.

In the high symmetry directions we measured, the elastic constants are related to the long wavelength phonon phase velocity

$$v=\lim_{q\to0}\frac{\omega}{|\vec{q}|}$$

as follows

100 direction

L-waves $\quad c_{11}/\rho=v_L^2(100)$

T-waves $\quad c_{44}/\rho=v_T^2(100)$

110 direction

L-waves $\quad (c_{11}+c_{12}+2c_{44})/2\rho=v_L^2(110)$

T_2-waves $\quad (c_{11}-c_{12})/2\rho=v_T^{2,2}(110)$.

Here ρ is the macroscopic crystal density.

To calculate zero sound elastic constants from our experimental data, we used all the frequencies higher than 1. rad THz, assuming that in the zero sound region we again find a constant gradient, thereby neglecting frequency dependent renormalisation effects in the zero sound region. It has been shown [23], that these effects are very small and well within the errors. In Table 2 we present the elastic constants in the zero sound region determined from our experiments at 295 K and compare them with first sound elastic constants measured by ultrasonic techniques. We extrapolated the ultrasonic data, where necessary, to 295 K using Haussühl's temperature gradient [17] and calculated the zero sound elastic constants separately for both experimental settings, the time-of-flight spectrometer with 2 m flight path and the more precise experimental set up with 4 m flight path. Due to the large corrections in the [100] TA branch because of the vertical divergence, we determined c_{44} from the high resolution measurements

only. The uncertainties assigned to the zero sound elastic constants reflect the uncertainties on the determination of the measured phonon frequencies.

There is a significant difference of the low and high frequency elastic constants c_{11} and $c''=(c_{11}-c_{12})/2$. However, the elastic constants c_{44} and c_{12} agree within the errors in the two regions.

In Table 3 we compare the calculated differences [4] with the experimental values. The mean values of the six ultrasonic measurements were subtracted from the mean values of our neutron studies. There is good agreement between theory and experiment in c_{11}, c_{44} and c''. However, theoretically a negative difference in c_{12} is expected, while the experimental value is about zero. These results are in agreement with other fcc Alkali Halides [1, 10] but they are in strong disagreement with results in the fcc rare gas solid Krypton, where near the triple point the largest effects in the order of 12 % occurred in c_{44} [24], as well as with the results in the molecular system adamantane where an effect of as much as 51 % occurs in c_{12}, while the difference between high and low frequency elastic constants c'' was -2.8 % [25]. From the analysis of our data, we believe that the large discrepancies in the zero and first sound elastic constants, especially c_{12} and c_{44}, derived by Raunio and Rolandson [8] at 80 K are over-estimated and might be due to the influence of the

Table 3. Calculated and experimental percentage difference between zero and first sound elastic constants in RbI at 295 K. The mean value of the six ultrasonic measurements was subtracted from the mean value of our neutron data. The calculated values are taken from Ref. [4]

	Δc_{11}	Δc_{44}	$\Delta(c_{11}-c_{12})/2$	Δc_{12}
Theory	9.5	1.4	14.6	-17.5
Exper.	9.7 ± 2	2.1 ± 3.5	10.9 ± 3.8	2.8 ± 13.8

vertical collimation, as these experiments were not specialized to the long wavelength low frequency region of the Brillouin zone. We calculated the difference between high and low frequency elastic constants in RbI at 80 K [23] and found Δc_{11} 2%, Δc_{44} 0.3%, and Δc_{12} −4%, while the experimental results were about Δc_{11} 10%, Δc_{44} 32%, and Δc_{12} 19% [8], model 1. We also analysed our out-of-symmetry data. For long-wavelengths the lattice dynamics of acoustic branches can be described by a long-wavelength approximation. In this approximation the dynamical matrix is given by

$$D_{\alpha\alpha}(\vec{q}) = (c_{11} - c_{44})\, q_\alpha^2$$
$$D_{\alpha\beta}(\vec{q}) = (c_{12} + c_{44})\, q_\alpha\, q_\beta \quad \alpha \neq \beta.$$

The frequencies ω are obtained from the following secular equation

$$|D_{\alpha\beta}(\vec{q}) + E\delta_{\alpha\beta}| = 0$$
$$E = \rho\,\omega^2 - c_{44}\,q^2.$$

In Figure 4 we compare the measured phonon phase velocities $|\omega/\xi|$ in the (100) plane from the $|\xi 00|$ to the $|\xi\xi 0|$ direction with the calculated first sound and zero sound phase velocities. All the data of this figure are taken from the high resolution measurements with 4 m flight-path. Again we used only data with frequencies larger than 1. THz and all the neutron groups were corrected for resolution effects as described in the previous chapter.
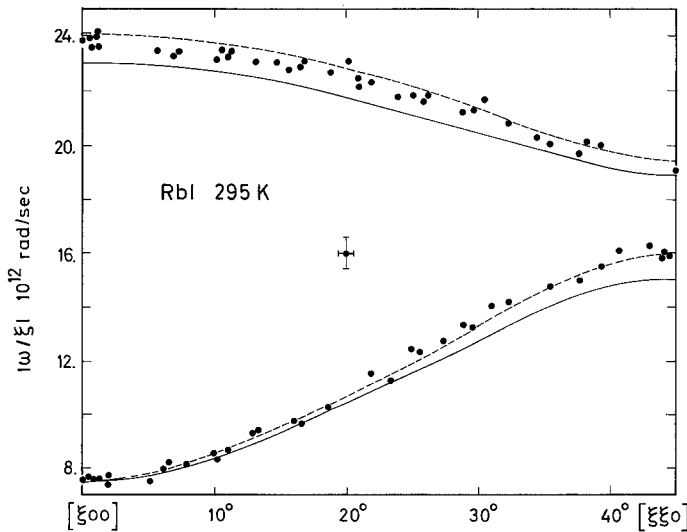

Fig. 4. Out of symmetry phonon phase velocities $|\omega/\xi|$. The neutron data of this work (●) are compared with the mean value of extrapolated ultrasonic data (————) and calculated zero sound phase velocities (----). The indicated error bar is a maximum error due to the smallest ξ-values used in the figure ($0.1 < \xi < 0.2$)
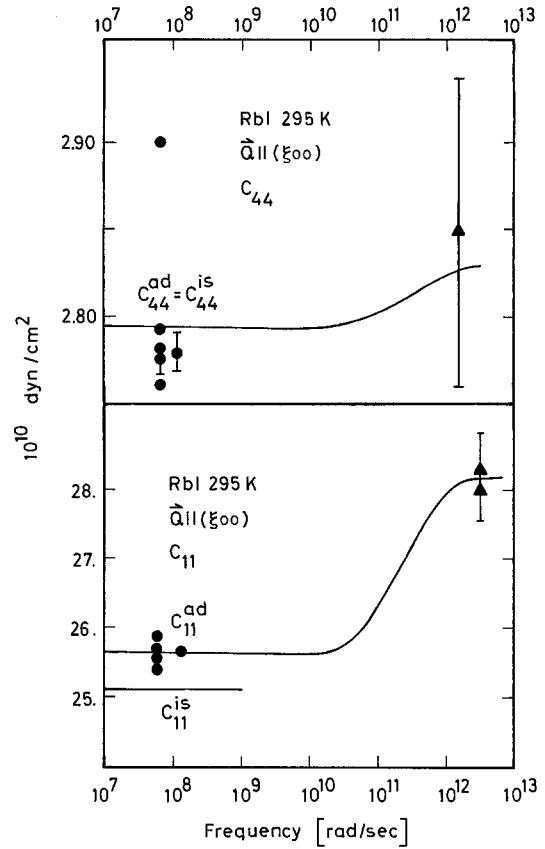

Fig. 5. Frequency dependence of the elastic constants c_{11} and c_{44}. The ultrasonic data (●) and our neutron data (▲) are compared with the calculated frequency dependence of Ref. [4] (————)

The theoretical zero sound "transverse" branch describes the measured data quite well. We see that near the $|\xi 00|$ direction zero sound and first sound are almost equal, while near the $|\xi\xi 0|$ direction there are significant differences. However, theoretically the zero sound phase velocities are slightly overestimated in the "longitudinal" branch.

In Figure 5 the theoretical frequency dependence of the elastic constants c_{11} and c_{44} [4] in the $|\xi 00|$ direction is shown and compared with the experimental ultrasonic data as well as with the high frequency values of this work. The elastic constant c_{11} shows a significant frequency dependence with a difference of the low and high frequency values of as much as 10%, which is far outside the experimental error bars. In c_{44} this effect is of the order of 2%, which is within the experimental uncertainties of both, the ultrasonic and the neutron data.

Conclusions

A considerable number of long-wavelength acoustic phonons in the (100)-plane of RbI has been measured

by time-of-flight inelastic neutron scattering. Though the collimations used for most experiments were better than typical collimations in triple axis spectrometry, we have shown that corrections of different types must be applied in order to deduce intrinsic peak positions. These corrections have been described in detail and it has been demonstrated that a numerical method involving a very simple long-wavelength approximation lattice dynamic model is sufficient to calculate not only peak-shifts but also lineshapes of observed neutron groups. An application of this method to data measured by triple axis spectrometers is in preparation.

From the properly corrected peak positions, zero sound elastic constants of RbI at room temperature have been derived and compared with theoretical calculations.

References

1. Cowley, R.C.: Proc. Phys. Soc. **90**, 1127–47 (1967)
2. Niklasson, G.: Phys. Kondens. Materie, **14**, 138–84, 1072
3. Cowley, R.A., Buyers, W.J., Svennson, E.C., Paul, G.L.: Neutron Inelastic Scattering IAEA, Vienna, p. 281–8 (1968)
4. Loidl, A., Jex, H., Daubert, J., Müllner, M.: phys. stat. sol (b) **76**, 581–92 (1976)
5. Buyers, W.J.L.: Phys. Rev. **153**, 923–30 (1976)
6. Dolling, G., Smith, H.G., Nicklow, R.M., Vijayaraghavan, P.R., Wilkinson, M.K.: Phys. Rev. **168**, 970–9 (1968)
7. Reid, J.S., Smith, T., Buyers, W.J.L.: Phys. Rev. **B1**, 1833–44 (1970)
8. Raunio, G., Rolandson, S.: phys. stat. sol. **40**, 749–57 (1970)
9. Svennson, E.C., Buyers, W.J.L.: Phys. Rev. **165**, 1063–6 (1968)
10. Loidl, A., Daubert, J., Schedler, E.: J. Phys. **C9**, L33–7 (1976)
11. Jex, H.: phys. stat. sol (b) **62**, 393–402 (1974)
12. Kress, W.: phys. stat. sol (b) **62**, 403–16 (1974)
13. Kress, W., Jex, H.: phys. stat. sol (b) **71**, 577–83 (1975)
14. Blaschko, O., Ernst, G., Quittner, G., Kress, W., Lechner, R.E.: Phys. Rev. **B11**, 3960–3965 (1975)
15. Gompf, F., Reichardt, W., Gläser, W., Beckurts, K.H.: Neutron Inelastic Scattering IAEA II, Vienna, p. 417–28 (1968)
16. Furrer, A.: Acta Cryst. **A27**, 461–70 (1971)
17. Haussühl, S.: Z. Physik **159**, 223–9 (1960)
18. Bolef, D.I., Menes, M.: J. Appl. Phys. **31**, 1010–7 (1960)
19. Reinitz, K.: Phys. Rev. **123**, 1615–9 (1961)
20. Lewis, J.T., Lehohoczky, A., Briscoe, C.V.: Phys. Rev. **161**, 877–87 (1967)
21. Chang, Z.P., Barsch, G.R.: J. Phys. Chem. Solids **32**, 27–40 (1971)
22. Gafhelehbashi, M., Dandekar, D.P., Ruoff, A.L.: J. Appl. Phys. **41**, 652–67 (1970)
23. Loidl, A.: Thesis Universität Frankfurt (1976)
24. Jackson, H.E., Landheer, D., Stoicheff, B.P.: Phys. Rev. Lett. **31**, 296–8 (1973)
25. Damien, J.C., Deprez, G.: Sol. Stat. Comm. **20**, 161–7 (1976)

A. Loidl
Institut für Physik
Johannes Gutenberg Universität Mainz
Jakob-Welder-Weg 11
D-6500 Mainz
Federal Republic of Germany

J. Daubert
Fachbereich Physik
Technische Universität München
D-8000 München
Federal Republic of Germany

M. Müllner
Institut für Kernphysik
Johann Wolfgang Goethe-Universität
Frankfurt/Main
August-Euler-Straße 6
D-6000 Frankfurt/Main 90
Federal Republic of Germany